Nonlinear Dynamics and Systems Theory, **20** (4) (2020) 374–387

Speed Sensorless Direct Torque Control Strategy of a Doubly Fed Induction Motor Using an ANN and an EKF

T. Djellouli [1,3], S. Moulahoum [2], A. Moualdia [2*], M.S. Bouchrit [1] and P. Wira [3]

[1] *Process Control Laboratory, National Polytechnic School, Algiers, Algeria*
[2] *Laboratory of Electrical Engineering and Automatics (LREA), University of Medea, Algeria*
[3] *IRIMAS , Laboratory of Modeling Intelligence Process Systems (MIPS), University of Haute Alsace, Mulhouse, France.*

Received: March 13 2020; Revised: September 18, 2020

Abstract: This study is devoted to the Direct Torque Control (DTC) strategy of a Doubly Fed Induction Motor (DFIM), with the use of an Artificial Neural Network (ANN) in the switching table, that gives the control sequence of the voltage inverter.This strategy is performed in two methods, the first one is with a mechanical sensor for the motor speed and, consequently, the position of its rotor, and the second one is without a mechanical sensor, using the Extended Kalman Filter (EKF) as a fast observer for the nonlinear closed loop with the obtained variable matrix. The EKF gives the new values of the state variables of the DFIM by minimizing the noise impact. This helps to avoid problems caused by the motor speed sensor and to make better the control robustness and its performances in the situation of any sensor fault. The selected configuration uses two voltage inverters linked to the stator and the rotor windings, which permits adopting the energy distribution between the stator and the rotor, and which is a suitable drive for the changeable speed application.

Keywords: *doubly fed induction motor (DFIM); direct torque control (DTC); artificial neural network (ANN); extented Kalman filter(EKF).*

Mathematics Subject Classification (2010): 03B52, 93C42, 94D05.

* Corresponding author: mailto:amoualdia@gmail.com

1 Introduction

In a generator system, the Double Feed Induction Machine (DFIM) is more used in different speed wind systems for electricity production [1], where in motor mode, it is found in high power applications such as traction, marine propulsion and pump storage systems [2, 3]. In this application, the DFIM works in motor operation, it is supplied by two Voltage Inverters (VI), one is for the stator and the second is for the rotor. This case is explained in Figure 1. The switching state of the VI is checked according to the counted values of the flux and the angle of this flux from the measured electrical amounts (voltages and currents). The switching table that gives the control sequence of the inverter is elaborated based on the ANN technique as the developed control ameliorates the torque reply by minimizing the oscillations compared to the conventional table control. The way exposed in this paper is the Direct Torque Control (DTC) which is applied to ensure a good dynamic performance and stability. The control is supported by the initial information on the flux, the rotor position and its fastness. In most cases, the latter is gained by a mechanical sensor. However, this demands a location installation that gives difficulty access or requires more space, decreases reliability in difficult environments and rises the expense of the machine. In this content, the Extended Kalman Filter (EKF) is used to estimate the speed of the DFIM as a work of the measured stator and rotor electrical variables [4].

This paper is organized as follows. Section 2 and Section 3 give, with no details, the modeling and control by DTC-ANN strategy of the DFIM with a speed sensor. Section 4 is dedicated to estimating the rotor speed by the EKF used in the evolved strategy. Section 5 introduces the simulation effects obtained by the application of the DTC-ANN strategy with and without a speed sensor. Concluding remarks are given in Section 6.

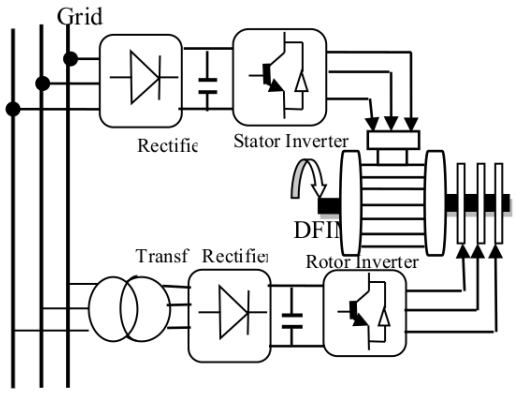

Figure 1: General schema of a DFIM powered by two Inverters.

2 Modeling of the DFIM

In order to achieve a good dynamic performance in DFIM control, it is necessary to have the model which represents the machine's behavior, not only in the permanent regimes, but also in the transient regimes. The modelling of the DFIM is based on the general equations in Concordia transformation applied on the stator and rotor windings, these

equations are given as follows [5]:

$$\begin{cases} V_{\alpha s} = R_s I_{\alpha s} + \frac{d\phi_{\alpha s}}{dt}, \\ V_{\beta s} = R_s I_{\beta s} + \frac{d\phi_{\beta r}}{dt}, \end{cases} \tag{1}$$

$$\begin{cases} V_{\alpha r} = R_r I_{\alpha r} + \frac{d\phi_{\alpha r}}{dt} + \omega\phi_{\beta r}, \\ V_{\beta r} = R_r I_{\beta r} + \frac{d\phi_{\beta r}}{dt} - \omega\phi_{\alpha r}, \end{cases} \tag{2}$$

$$\begin{cases} \phi_{\alpha s} = L_s I_{\alpha s} + M I_{\alpha r}, \\ \phi_{\beta s} = L_s I_{\beta s} + M I_{\beta r}, \end{cases} \tag{3}$$

$$\begin{cases} \phi_{\alpha r} = M I_{\alpha s} + L_r I_{\alpha r}, \\ \phi_{\beta r} = M I_{\beta s} + L_r I_{\beta r}, \end{cases} \tag{4}$$

where ω_s, ω are the stator and rotor pulsations, $\omega = p\Omega$. Ω is the mechanical rotating speed. The angular relationship is defined by Figure 2 [6]:

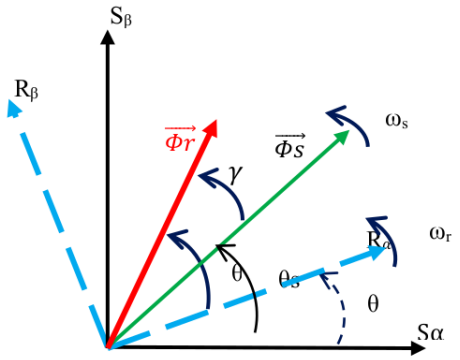

Figure 2: Stator and rotor flux position in the DFIM.

$$\theta_s = \theta_r + \theta - \gamma, \tag{5}$$

θ_s : Angular position of the rotating reference $\alpha - \beta$,
θ_r : Angular position relative to α axis,
θ : The electrical angular position of the rotor relative to the stator reference frame.
So, in the steady state ($d\gamma/dt = 0$) and with

$$\begin{cases} \frac{d\theta_s}{dt} = \omega_s, \\ \frac{d\theta}{dt} = \omega, \\ \omega_s = \omega + \omega_r, \end{cases} \tag{6}$$

the dynamical equation is given by

$$J\frac{d\Omega}{dt} = T_{em} - T_r - K_f\Omega \tag{7}$$

and the electromagnetic torque equation is

$$T_{em} = \frac{P \cdot M}{L_r}\left(\Phi_{\alpha r} I_{\beta s} - \Phi_{\beta r} I_{\alpha s}\right). \tag{8}$$

The motor is powered directly by two three-phase voltage inverters, as it is represented in Figure 1.

3 Strategy Applied on DFIM

The system, studied in this work, is the DFIM powered by two voltage inverters (VI) for the stator and the rotor, Fig.1. The switching states of the inverters are generated using a direct torque control (DTC) strategy, where the current and voltage sensors are needed [7]. The DTC makes it possible to control the optimum electromagnetic torque from the flow metrics and their positions. The main advantages of the DTC applied to the induction machine are:

- The DTC has a simple structure and a robust control, if one ensures a good quality of the estimation of the flows during operation, and consequently, a good estimate of the couple.

- The DTC with two ST (switching tables) provides excellent torque dynamics, but the positions of the stator and rotor flows and the angle between these fluxes must be carefully controlled. In this paper, a separate control of the stator and rotor flows is proposed. In order to apply the DTC strategy to two voltage inverters on the DFIM, we define a first ST to control the stator flux vector and a second ST to control the rotor flux vector. The next part of the control strategy controls the interaction between the two streams. As a result, it is possible to regulate the speed as long as the electromagnetic torque is controllable [7].

By using the stator flux $\vec{\Phi}_s$ and the rotor flux $\vec{\Phi}_r$ vectors as state variables, the DFIM electromagnetic torque can be expressed as follows [7, 8]:

$$\begin{cases} \overrightarrow{T_{em}} = \frac{3}{2} \cdot \frac{PM}{\sigma_s L_r} \left(\vec{\Phi}_s \wedge \vec{\Phi}_r \right), \\ \|T_{em}\| = K \cdot \left(\left\| \vec{\Phi}_s \right\| \cdot \|\overrightarrow{\Phi_r}\| \right) \cdot \sin(\gamma), \end{cases} \tag{9}$$

where P is the number of pole pairs, L_s, L_r are the stator and rotor self-inductances, M is the mutual inductance, and $\sigma = 1 - \frac{M}{L_s L_r}$ is the dispersion coefficient. $\vec{\Phi}_s$ and $\vec{\Phi}_r$ are the stator and rotor flux space vectors and γ is the angle between the fluxes as shown in Figure 2. The constant $'K'$ is defined as below:

$$\mathrm{K} = \frac{3}{2} \cdot \frac{\mathrm{PM}}{\sigma \mathrm{L_s L_r}}. \tag{10}$$

By analyzing relation (9), two strategies can be proposed for the torque control:

- by fixing the flux module and adjusting the γ angle,

- by fixing the γ angle and adjusting the flux module.

In this study, the authors [6, 7] chose the first strategy. The DTC strategy applied to this system will provide fast and robust torque and flux responses.

3.1 Stator and rotor inverter control

The first inverter is connected to the stator winding (Stator Inverter (SI)), and the second one is connected to the rotor winding (Rotor Inverter (RI)), S_1, S_2, and S_3 are the switching sequence sent to the IGBT gates. The instantaneous value of the stator flux and its position are estimated from the measured electrical quantities. Using hysteresis comparators, the flux and the position are controlled directly and independently with an appropriate selection of the voltage vector imposed by the inverter. The inverter provides eight voltage vectors. These vectors are chosen by a switching table based on the errors of flux and its position. Table 1 is deduced according to the switching sequence from the model of the induction machine in a stationary reference and the expression of the stator voltage.

Table 1. Voltage Inverter Table.

voltage vector	S_1	S_2	S_3	V_{ab}	V_{bc}	V_{ca}
V_0	0	0	0	0	0	0
V_1	1	0	0	+U	0	−U
V_2	1	1	0	0	+U	−U
V_3	0	1	0	−U	+U	0
V_4	0	1	1	−U	0	+U
V_5	0	0	1	0	−U	+U
V_6	0	1	0	+U	−U	0
V_7	1	1	1	0	0	0

The stator flux is estimated from the following relation:

$$\Phi_s(t) = \int (V_s - R_s I_s)\, dt. \tag{11}$$

Over the time interval $[0, T_s]$, corresponding to a sampling period T_e, it is considered that the term $R_s I_s$ is negligible compared to the voltage V_s, thus

$$\Phi_s = \Phi_{s0} + V_s T_e. \tag{12}$$

The stator and rotor flux vectors can be estimated directly into the stator and rotor voltage vectors

$$\begin{cases} \frac{d}{dt}\vec{\phi}_s = \vec{V}_s, \\ \frac{d}{dt}\vec{\phi}_r = \vec{V}_r. \end{cases} \tag{13}$$

We integrate (11) during a sampling period T_e. Thus, the following equation is obtained:

$$\begin{cases} \overline{\Phi_s\,(t_{n+1})} = \overline{\Phi_s\,(t_n)} + T_e \cdot \overline{V_s\,(t_n)}, \\ \overline{\Phi_r\,(t_{n+1})} = \overline{\Phi_r\,(t_n)} + T_e \cdot \overline{V_r\,(t_n)}. \end{cases} \tag{14}$$

The voltage vector application time is T_e. Consequently, V_s and V_r remain constant during the time interval $[t_n, t_{n+1}]$, where $t_{n+1} = t_n + T_e$. Equation (8) can be rewritten as

$$\begin{cases} \overline{\Phi_s^{n+1}} = \overrightarrow{\Phi_s^n} + T_e \cdot \overrightarrow{V_s^n}, \\ \Phi_r^{n+1} = \overrightarrow{\Phi_r^n} + T_e \cdot V_r^n. \end{cases} \tag{15}$$

For each sampling time, the appropriate output voltage vector of the inverter can be deduced from the estimated values of the flux. In Figure 3, six sectors are defined in the stationary reference frame (α, β). Therefore, if θ_s (or θ_r) is in the same sector, the use of an identical voltage vector leads to a similar phase and amplitude evolution of the flux vector. The rotor flux vector is defined in the same way [6]. Thus, the applied voltage

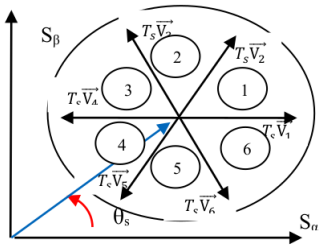

Figure 3: Applicable voltage vectors for the stator flux vector control.

vectors depend on the following:

1. The sector number (according to θ_s and θ_r).

2. The required flux angular position.

3. The required flux magnitude evolution.

This is illustrated in ST shown in Table 2. Two independent STs are implemented in the control system. They allow controlling the rotor and stator fluxes. The DTC strategy is aimed to separate the stator and rotor flux adjustment. In this way, the flux interaction is controlled, and consequently, the electromagnetic torque T_{em}(13).

Table 2. Switch positions and their voltage vectors

		Sector number N					
$\vec{\Phi}$ evolution		1	2	3	4	5	6
$\|\vec{\Phi}\|$	θ	Voltage vector					
↗	↗	V_2	V_3	V_4	V_5	V_6	V_1
↗	↘	V_6	V_1	V_2	V_3	V_4	V_5
↘	↗	V_3	V_4	V_5	V_6	V_1	V_2
↘	↘	V_5	V_6	V_1	V_2	V_3	V_4

3.2 DTC-ANN applied on DFIM

The proposed DTC-ANN consists to replace the switching table which provides the voltage vector, the Artificial Neural Network (ANN) switching table inputs are:

- $\Delta\Phi s$ The flux error.
- $\Delta\Phi r$: The angle error.

N_s is the number of sector from 1 to 6. This ANN is based on forward-forward propagation with three hidden layers having, respectively [4, 14], 16 neurons in each layer and one connection as activation functions. The output layer has three neurons providing a voltage vector [9], the proposed ANN switching table is shown in Figure 4. It is well

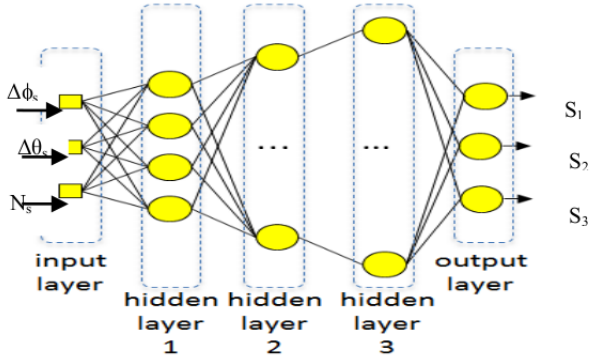

Figure 4: The ANN structure for switching table.

known that the stator windings and the rotor windings are fed by two three-phase systems where the rotor current frequency has a slip. The angular relation of rotor can be deduced as (Figure 2):

$$\theta_r = \gamma + \theta_s - \theta. \tag{16}$$

The global scheme of the proposed control strategy is illustrated in Figure 5. In this diagram, Ω is the mechanical rotation speed measured by a sensor installed on the rotor.

4 Speed Sensorless Control by EKF

The rotor position and DFIM speed data are indispensable in the check. They are always obtained via a mechanical speed sensor. But, this sensor needs a place for its installation, moreover, this leads to some problems in its installation; and it is affected by noises and vibrations. Various techniques have been proposed in the literature to remove this mechanical sensor. Among these techniques, there is the speed estimation using the EKF. This Kalman filter is an observer for the nonlinear closed loop with the obtained variable matrix. In every calculation stage, the Kalman filter gives the new values of the state variables of the DFIM. The prediction values are made by minimizing the noise impact and modeling the parameter faults or the unstable state. Noises are supposed to be white, Gaussian and not correlated with the estimated states [10].

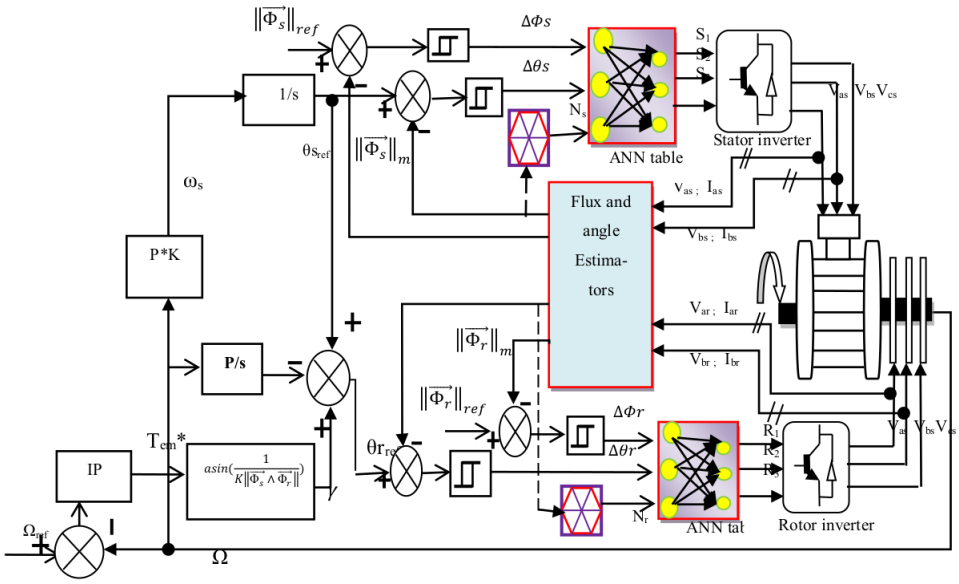

Figure 5: Global block diagram of the DTC with a mechanical speed sensor.

4.1 Selection of DFIM model

We consider the angular rotor speed ω as a state variable which increases the size of the state vector, in this case, this state vector becomes

$$x = [i_{\alpha s} \quad i_{\beta s} \quad i_{\alpha r} \quad i_{\beta r} \quad \omega]^T, \tag{17}$$

$$u = [v_{\alpha s} \quad v_{\beta s} \quad v_{\alpha r} \quad v_{\beta r}]^T. \tag{18}$$

The time-domain of the motor model is given as[11]:

$$\dot{x} = f(x,u) = Ax + Bu, \tag{19}$$

$$y = h(x) = [i_{\alpha s} i_{\beta s}]^T, \tag{20}$$

$$A = \begin{bmatrix} -\frac{R_S}{\sigma L_S} & \frac{(1-\sigma)}{\sigma}\omega & \frac{R_r M}{\sigma L_s L_r} & \frac{M}{\sigma L_S}\omega \\ -\frac{(1-\sigma)}{\sigma}\omega & -\frac{R_S}{\sigma L_S} & -\frac{M}{\sigma L_S L_r}\omega & \frac{R_r M}{\sigma L_S L_r} \\ \frac{R_S M}{\sigma L_s L_r} & \frac{-M}{\sigma L_r}\omega & -\frac{R_r}{\sigma L_r} & -\frac{1}{\sigma}\omega \\ \frac{M}{\sigma L_r}\omega & \frac{R_S M}{\sigma L_S L_r} & \frac{1}{\sigma}\omega & -\frac{R_r}{\sigma L_r} \end{bmatrix}, \tag{21}$$

$$B = \begin{bmatrix} \frac{1}{\sigma L_s} & 0 & -\frac{M}{\sigma L_s L_r} & 0 \\ 0 & \frac{1}{\sigma L_s} & 0 & -\frac{M}{\sigma L_s L_r} \\ -\frac{M}{\sigma L_s L_r} & 0 & \frac{1}{\sigma L_r} & 0 \\ 0 & -\frac{M}{\sigma L_s L_r} & 0 & \frac{1}{\sigma L_r} \end{bmatrix}, \tag{22}$$

$$\mathrm{C} = \begin{bmatrix} 1 & 0 & 0 & 0 & 0 \\ 0 & 1 & 0 & 0 & 0 \end{bmatrix}. \tag{23}$$

The above equations can be written also as

$$\frac{d}{dt}\begin{bmatrix} I_{\alpha s} \\ I_{\beta s} \\ I_{\alpha r} \\ I_{\beta r} \\ \omega \end{bmatrix} = \begin{bmatrix} a_1 & a_2 p\Omega & a_3 & a_4 p\Omega & 0 \\ -a_2 p\Omega & a_1 & -a_4 p\Omega & a_3 & 0 \\ a_5 & -a_6 p\Omega & a_7 & -a_8 p\Omega & 0 \\ a_6 p\Omega & a_5 & a_8 p\Omega & a_7 & 0 \\ 0 & 0 & 0 & 0 & 1 \end{bmatrix} \begin{bmatrix} I_{\alpha s} \\ I_{\beta s} \\ I_{\alpha r} \\ I_{\beta r} \\ \omega \end{bmatrix} + Bu \tag{24}$$

with

$$Bu = \begin{bmatrix} b_1 & 0 & b_2 & 0 \\ 0 & b_1 & 0 & b_2 \\ b_2 & 0 & b_3 & 0 \\ 0 & b_2 & 0 & b_3 \\ 0 & 0 & 0 & 0 \end{bmatrix} \begin{bmatrix} V_{\alpha s} \\ V_{\beta s} \\ V_{\alpha r} \\ V_{\beta r} \end{bmatrix}, \tag{25}$$

$$\begin{bmatrix} I_{\alpha s} \\ I_{\beta s} \end{bmatrix} = \begin{bmatrix} 1 & 0 & 0 & 0 & 0 \\ 0 & 1 & 0 & 0 & 0 \end{bmatrix} [\ I_{\alpha s} \quad I_{\beta s} \quad I_{\alpha r} \quad I_{\beta r} \quad \omega]^T, \tag{26}$$

where the parameters a_i and b_i are given by

$$a_1 = -\tfrac{R_s}{\sigma L_s}, a_2 = \tfrac{(1-\sigma)}{\sigma}, a_3 = \tfrac{R_r M}{\sigma L_s L_r}, a_4 = \tfrac{M}{\sigma L_s}, \tag{27}$$

$$a_5 = \tfrac{R_s M}{\sigma L_s L_r}, a_6 = \tfrac{-M}{\sigma L_r}, a_7 = -\tfrac{R_r}{\sigma L_r}, a_8 = \tfrac{1}{\sigma}, \tag{28}$$

$$b_1 = \tfrac{1}{\sigma L_s}, b_2 = -\tfrac{M}{\sigma L_s L_r}, \quad b_3 = \tfrac{1}{\sigma L_r}. \tag{29}$$

4.2 DFIM discretization model

The DFIM discrete state space model is obtained from equations (23) and (24) as follows [10, 12]:

$$X_{k+1} = f(X_k, U_k) = A_k X_k + B_k U_k, \tag{30}$$

$$Y_k = h(X_k) = C_k X_k, \tag{31}$$

where A_k ,B_k and C_k are the discredited system matrix, input matrix and output matrix, respectively, thus

$$\begin{cases} A_k = 1 + TA, \\ B_k = \mathrm{BT}, \\ C_k = \mathrm{C}, \end{cases} \tag{32}$$

where T is the sampling time and I is an identity matrix.

$$\begin{cases} A_k = \begin{bmatrix} 1 + a_1 T & a_2 p\Omega \mathrm{T} & a_3 T & a_4 p\Omega \mathrm{T} & 0 \\ -a_2 p\Omega \mathrm{T} & 1 + a_1 T & -a_4 p\Omega \mathrm{T} & a_3 T & 0 \\ a_5 T & -a_6 p\Omega \mathrm{T} & 1 + a_7 T & -a_8 p\Omega \mathrm{T} & 0 \\ a_6 p\Omega \mathrm{T} & a_5 T & a_8 p\Omega \mathrm{T} & 1 + a_7 T & 0 \\ 0 & 0 & 0 & 0 & 1 \end{bmatrix}, \\ B_k = T \begin{bmatrix} b_1 & 0 & b_2 & 0 \\ 0 & b_1 & 0 & b_2 \\ b_2 & 0 & b_3 & 0 \\ 0 & b_2 & 0 & b_3 \\ 0 & 0 & 0 & 0 \end{bmatrix}, \\ C_k = \begin{bmatrix} 1 & 0 & 0 & 0 & 0 \\ 0 & 1 & 0 & 0 & 0 \end{bmatrix}, \end{cases} \tag{33}$$

$$X_k = \begin{bmatrix} I_{\alpha s}(k) \\ I_{\beta s}(k) \\ I_{\alpha r}(k) \\ I_{\beta r}(k) \\ \omega(k) \end{bmatrix}, \; X_{k+1} = \begin{bmatrix} I_{\alpha s}(k+1) \\ I_{\beta s}(k+1) \\ I_{\alpha r}(k+1) \\ I_{\beta r}(k+1) \\ \omega(k+1) \end{bmatrix}, \; U_k = \begin{bmatrix} V_{\alpha s}(k) \\ V_{\beta s}(k) \\ V_{\alpha r}(k) \\ V_{\beta r}(k) \end{bmatrix}. \tag{34}$$

Let v be the noise vector of the system which perturbs the state vector, and w be the measurement noise vector which perturbs the measurement vector [11]

$$\begin{cases} X_{k+1} = f\left(X_k, U_k\right) + w_k, \\ Y_k = h\left(X_k\right) + v_k. \end{cases} \tag{35}$$

The Kalman filter considers the system noise vector and the measurement noise vector as the Gaussian white noise of zero mean, which is free of the basic state vector and their covariance matrices, these are, respectively, Q and R, defined by

$$\begin{cases} Q = \mathrm{cov}(w) = E\left\{ww^T\right\}, \\ R = \mathrm{cov}(v) = E\left\{vv^T\right\}. \end{cases} \tag{36}$$

4.3 Determination of the noise and state covariance matrices

To obtain the best considerable speed value, it is necessary to use exact initial values for the covariance system matrices of the noise measurement and the state noise Q, R and P, respectively [12].They have important results on the stability filter and convergence time. These matrices are supposed to be matrices of diagonal covariance.

4.4 Implementation of the discretized EKF algorithm

The filtering algorithm is formed of two major steps, a prediction step and a filtering step [10, 11].

- ϒ In the prediction process, the following predicted states values $\widehat{X}(\boldsymbol{k+1})$ are got by using a mathematical model (state-variable equations), also the former values of the estimated states. Therefore, the predicted state covariance matrix (P) is gained before the new measurement values. At the end, the mathematical model and also the covariance matrix of the system (Q) are used.

- ϒ During the second step, which is the filtering step, the following estimated states, $\hat{X}(k+1)$, are got from the predicted ones, they estimate $X(k+1)$ by adding a correction term $K(y-\hat{y})$ to the predicted value.

This correction term is a weighted variety between the current output vector (y) and the predicted output vector ($\hat{y}$). Here K is the Kalman gain. The estimated states are gained from the following stages [13, 14].

- Initialization of the state vector and covariance matrices.
- Prediction of the state vector

$$\hat{X}_{k+1/k} = f\left(X_{k/k}, U_k\right). \tag{37}$$

- Covariance estimation of prediction.

- Kalman filter gain computation.
- Covariance matrix of estimation error.

Finally, the global scheme of the proposed control strategy is illustrated in Figure 6.

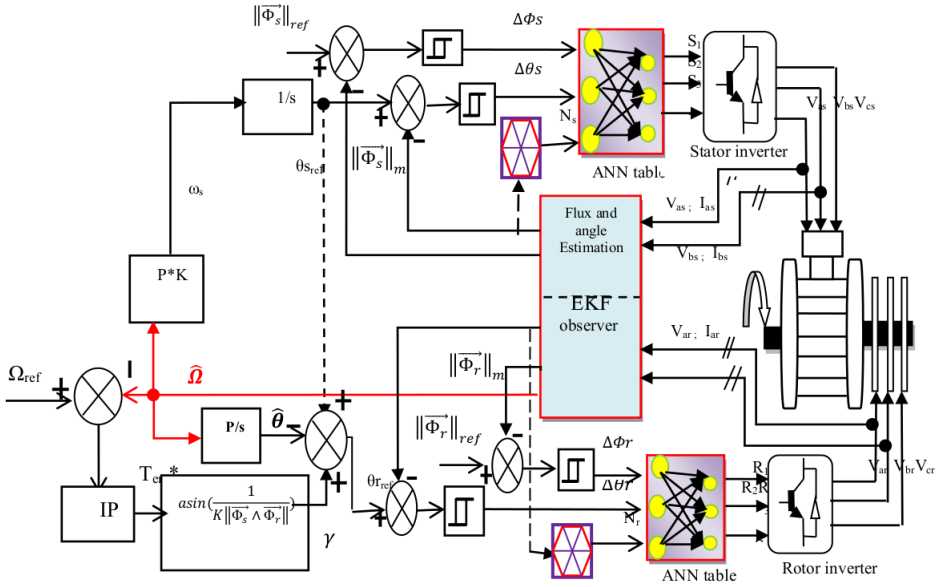

Figure 6: Global block diagram of the DTC without speed sensor by the EKF observer.

5 Results and Discussion

The DFIM in this work is: 4kW; 220/380V − 50Hz 15/8.6A; 1440rpm whose nominal parameters are reported in the Appendix. The simulations of the DFIM control and speed estimation method with the extended Kalman filter have been done using the MATLAB/Simulink software. An Artificial Neural Network (ANN) switching table and a Classical Integral Proportional(IP) controller were used for the speed control and direct torque control. Simulation results are shown in Figure 7. Figure 7(a) represents the speed response using the mechanical sensor after applying a step at (t = 0.1s); then the load torque application at (t = 0.5s). After that the reversal of the rotation direction at (t = 1s). Figure 11(b) presents the same answer estimated speed by EKF, it shows also the speed measured by the sensor and that estimated (without the sensor). Both curves coincide and follow very well the reference, especially in the steady state. Almost the same evolution of the magnitudes is noted: Electromagnetic torque in Figure 11(c) and (d); Stator Currents in Figure 7 (e) and (f); Stator flux circle and rotor flux circle in Figure 7 (g) and (h). Except in the case of a sensorless control, there is a small fluctuation due to the estimation by the Kalman filter. These results are shown in diagram, we develop a speed sensorless DTC strategy of a DFIM using the EKF, eliminating the mechanical speed sensor. Note that the EKF estimator presents a good tracking for the rotor speed with a negligible error in steady state, the EKF is still robust during the load application and reversal of the motor speed.

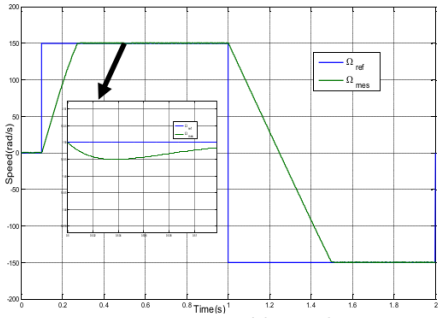

(a) Speed step response with speed sensor

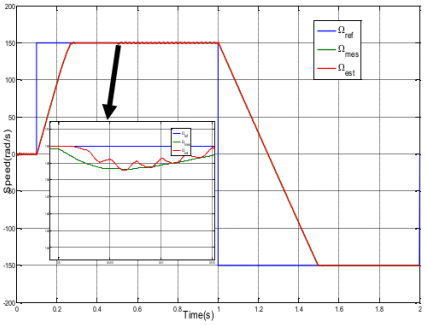

(b) Speed step response without speed sensor

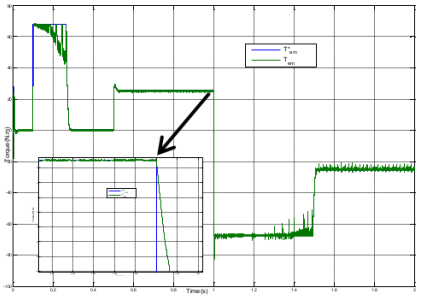

(c) Electromagnetic Torque with speed sensor

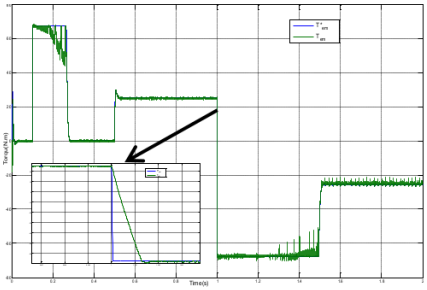

(d) Electromagnetic Torque without speed sensor

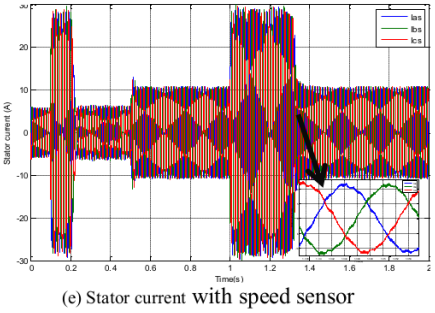

(e) Stator current with speed sensor

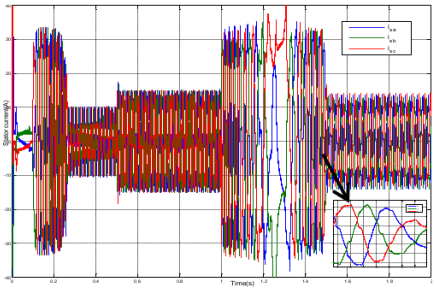

(f) Stator current without speed sensor

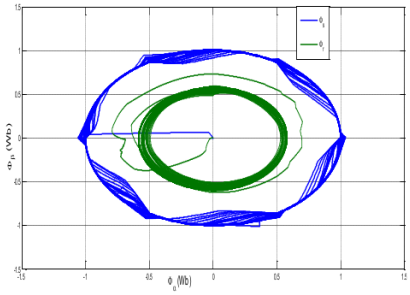

(g) Stator flux circle and rotor flux circle with speed sensor

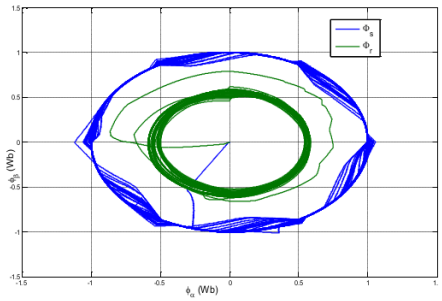

(h) Stator flux circle and rotor flux circle without speed sensor

Figure 7: Simulation results.

6 Conclusion

In this paper, the direct torque control strategy by two switching tables developed by ANN technique applied on DFIM, with and without a mechanical sensor, is presented. In order to guarantee a good dynamic performance of the overall system and to solve the problem of control, accompanied generally with the mechanical sensor fault, the EKF approach is used as a speed observer in the DTC, which makes it possible to obtain a good control for the voltages generated by the inverters, and consequently, a good metric of flux and torque, in order to ensure a good dynamic performance of the controlled system without a mechanical speed sensor. The results obtained show a good regulation of the electrical and magnetic quantities, which ensures the efficiency of this strategy without a speed sensor and the stability of the system in the event of load or sensor fault.

Acknowledgment

The research is part of a project PRFU'2020, realized, respectively, in the Laboratory of Process Control (LCP), National Polytechnic School, Algiers, Algeria, and Laboratory of Electrical Engineering and Automatic LREA Research, University of Medea.

References

[1] T. Douadi, Y. Harbouche, R. Abdessemed and I. Bakhti. Improvement Performances of Active and Reactive Power Control Applied to DFIG for Variable Speed Wind Turbine Using Sliding Mode Control and FOC. *International Journal of Engineering TRANSACTIONS A* **31**(10) (2018) 1689–1697.

[2] D. Ben Attous and Y. Bekakra. Speed Control of a Doubly Fed Induction Motorusing Fuzzy Logic Techniques. *International Journal on Electrical Engineering and Informatics* **2** (3) (2010) 179–191.

[3] S. Khojet El Khil, I. Slama-Belkhodja, M. Pietrzak-David and B. de Fornel. A Fault Tolerant Operating System in a Doubly Fed Induction Machine Under Inverter Short-circuit Faults. *32nd Annual Conference on IEEE Industrial Electronics, Paris, France*, Nov. (2006).

[4] M. Abdelrahem, C. Hackl and R. Kennel. Application of Extended Kalman Filter to Parameter Estimation of Doubly-Fed Induction Generators in Variable-Speed Wind Turbine Systems. *International Conference on Clean Electrical Power(ICCEP)* (2015) 226–233.

[5] S. Lekhchine, T. Bahi, I. Aadlia, Z. Layateb and H. Bouzeria. Speed control of doubly fed induction motor. *Energy Procedia* **74** (2015) 575–586.

[6] F. Bonnet, P.E. Vidal and M. Pietrzak-David. Dual Direct Torque Control of Doubly Fed Induction Machine. *IEEE Transactions on Industrial Electronics* **54** (5) (2007) 2482–2490.

[7] M. Abdellatif, M. Debbou, I. Slama-Belkhodja and M. Pietrzak-David. Simple Low-Speed Sensorless Dual DTC for Double Fed Induction Machine Drive. *IEEE Transactions on Industrial Electronics* **(61)** (8) (2014) 3915–3922.

[8] F. Bonnet and M. Pietrzak-David. Control optimization of a doubly fedinduction machine. *IEEE Power Electronics Specialists Conference, Rhodes* (Jun 2008) 2579–2585.

[9] C. Kamal Basha and M. Suryakalavathi. Estimation of Rotor Flux using Neural Network Observer in Speed Sensorless Induction Motor Drive. *International Journal of Computer Applications* **79** (6) (2014).

[10] M. Vafaie, B. Dehkordi, P. Moallem and A. Kiyoumarsi. Minimizing Torque and Flux Ripples and Improving Dynamic Response of PMSM using a Voltage Vector with Optimal Parameters. *Industrial Electronics IEEE Transactions* **63** (2015) 3876–3888.

[11] H. Hamidi and A. Valizadeh. Improvement of Navigation Accuracy using Tightly Coupled Kalman Filter. *International Journal of Engineering TRANSACTIONS B: Applications* **30**)(2) (2017) 215–223.

[12] Y-R. Kim, S-K. Sul and M-H. Park. Speed sensorless vector control of induction motor using extended Kalman filter. *IEEE Transactions on Industry Applications* **30** (05) (1994) 1225–1233.

[13] K.C. Wong, S.L. Ho and K.W.E. Cheng. Direct torque control of a doublyfed induction generator with space vector modulation. *Elec. Pow. Comp. and Syst.* **36**(12) (2008) 1337–1350.

[14] Y. Chedni, D.J. Boudana, A. Moualdia, L. Nezli and P. Wira. Sensorless Two Series Connected Quasi Six-Phase IM Based Direct Torque Control for Torque Ripples Minimization. *Nonlinear Dynamics and System Theory* **20**(2) (2020) 153–167.

[15] A. Moualdia, M. O. Mahmoudi and L. Nezli. Direct Torque Control of the DFIG and Direct Power Control for Grid Side Converter in wind power generation system. *The Mediterranean Journal of Measurement and Control, MEDJMC* **9**(3) (2013) 101–108.

[16] S. Boulkhrachef, A. Moualdia, Dj. Boudana and P. Wira. Higher-order sliding mode control of a wind energy conversion system.*Nonlinear Dynamics and System Theory* **19**(4) (2019) 486–496.

[17] A. Chalanga, S. Kamal and B. Moreno. I mplementation of super-twisting control: supertwisting and higher Order sliding-mode observer-based approaches. *IEEE Trans. on Industrial Electronics* **63**(6) (2016) 3677–3685.

[18] A.G. Mazko. Robust output feedback stabilization and optimization of discrete-time control systems. *Nonlinear Dynamics and System Theory* **18**(1) (2018) 92–106.

[19] E. Benyoussef, A. Meroufel and S. Barkat. Neural network and fuzzy logic direct torque control of sensorless double star synchronous machine. *Rev. Roum. Sci. Techn. Ectrotechn. et Nerg.* **61**(3) (2016) 239–243.

APPENDIX

Table 3. DFIM parameters used in simulation.

Stator resistance	$Rs = 1.2\Omega$
Rotor resistance	$Rr = 1.8\Omega$
Stator inductance	$Ls = 0.1554H$
Rotor inductance	$Lr = 0.1554H$
mutual inductance	$M = 0.15H$
Inertia moment	$J = 0.07Kg.m^2$
Coefficient of viscous friction	$f = 0.001$
Number of pairs of poles	$P = 2$